

Nano Additives in Cashew Nut Shell Liquid Biodiesel and Environment Emissions of Diesel Engine

Deepak Kumar^{*}, Vijay Kumar Chhibber², Ajay Singh³

¹ Research Scholar, Department of Chemistry, Uttarakhand Technical University, Dehradun, India

² Indian School of Petroleum (IIP), Dehradun & Dean Baba Farid Institute of Technology, Dehradun, India

³ Department of Chemistry, Uttaranchal University, Dehradun, India

Corresponding author email: kumar.deepbt@gmail.com

<https://doi.org/10.14447/jnmes.v25i2.a01>

Received: January 2-2022

Accepted: March 17-2022

Keywords:

Cashew Nut Shell Liquid (CNSL), CO Emissions, CO₂ Emissions, FTIR, GCMS Analysis, Hydrocarbon Emissions, NO_x Emissions

ABSTRACT

The developing countries are using non-edible oils for the production of biofuels, additives, or alternate fuels. The research article focused on the behavior study and analysis of cashew nut shell liquid (CNSL) biodiesel obtained by processing the cashew nut shell liquid. The work is carried out to derive the thermal-cracked (TC) -CNSL oil from Cardanol in the temperature range 150°C to 400°C. The chemical functional groups are studied using Fourier-transform infrared spectroscopy (FTIR) and gas chromatography-mass spectrometry (GCMS) techniques. The TC-CNSL blended fuel performance is compared with diesel and neat biodiesel (B-100). The physicochemical properties of diesel, CNSL, and TC-CNSL biodiesel are estimated based on American Society for Testing and Materials (ASTM) standards. The 50 parts per million (ppm) Cerium Oxide Nanoparticles are added with TC-CNSL-B25, TC-CNSL-B50, TC-CNSL-75, and TC-CNSL-B100 and processed in a single stroke diesel engine working at constant speed 1500-rpm. The blended fuel is analyzed based on environmental emission parameters in the diesel engines. The carbon monoxide (CO), carbon dioxide (CO₂), hydrocarbon (HC) emissions of B-100 are reduced by 40.5 %, 60.9 %, and 30.7 % respectively in comparison to diesel, at full load. The nitrogen oxide (NO_x) emissions are increased by 13.26 % in B-100 in comparison to diesel, at full load. The smoke density is also observed decreasing in B-100 in comparison to diesel.

1. INTRODUCTION

Vegetable oils are the major sources of renewable energy, considered as the promising solution to diesel fuel [1]. Many developing countries are using biodiesel because of its features of environment friendly, renewable, non-toxic, and biodegradable. Biodiesel is having good lubricity, lower volatility, lower sulfur, good calorific value, oxygen content, and cetane index in comparison to conventional diesel fuel [2-3]. Karanja, Mahua, neem, rapeseed, rice bran, jatropa [4-5] castor, sal, cashew nut, soybean, sunflower, etc. are a few vegetable seeds [6-7] used for biodiesel production and lubricants [8].

The cashew tree or *Anacardium Occidentale* [9] produces the cashew apple and cashes weeds, used for oil extraction. The fruits of the cashew are widely used for eating. It is used in many food recipes, including cheeses, butter, and liquor. The cashew shell oil or cashew nut shell liquid (CNSL) [10] is a natural oil in yellowish color, a byproduct of cashew nuts having a honeycomb structure. The composition of the oil depends on the quantity used for processing. The CNSL consists of alkyl-substituted phenolic structures, and the molecules show antioxidants [11] due to their compounds. The oil can be processed using a hot oil processing method to extract the solvents. The composition of normal CNSL contains anacardic acid, cardol, cardanol, and 2-methyl-cardol [12]. The CNSL consist of anacardic acids (60-70 %), cardol (10-20 %), cardanol (5-10 %) and 20 methyl-cardol (2-5%). The heat treatment of CNSL provides 8% cardol and 78%

cardanol that can degrade the degree of polymerization for the contents present in cashew oil and unsaturated alkyl-phenols. Cardanol is used in chemical industries for coatings, friction materials, and resins.

The cashew nut is available in most of the south and west regions of India. The cashew nut is cultivated on 0.817 million-ton hectares (MT-Ha) land in different states of India. The data of Horticulture Statistics Division, Department of Agriculture, Crop & Farmers Welfare (2017-2018), reveals that different states in India use the agriculture land (million-ton hectares), to produce cashew nut: Andhra Pradesh (0.11692), Assam (0.00113), Chhattisgarh (0.00983), Gujarat (0.00650), Jharkhand (0.00613), Karnataka (0.08945), Kerala(0.08818), Maharashtra(0.26944), Manipur (0.00032), Meghalaya (0.00612), Nagaland (0.00054), Odisha (0.09859), Tamil Nadu (0.07103), Tripura(0.00345), West Bengal (0.01296), and others (0.03642). Many researchers have reported that the waste products can be used as an alternative or additives in a diesel engine. CNSL is one of the substitutes in diesel engines apart from animal fats, other vegetable oils, plastic oils that are majorly used in developing countries such as India. The cashew nutshell is a great source of biomass, available at low cost, can be used as a substitute in CI engine and vehicle transportation [13].

Cashew shell and cashew shell cake [14] both have two different biomaterials based on thermogravimetric profiling. The vacuum pyrolysis method is also used to extract the cashew nut shell liquid. The distillation process was used to minimize polymeric material. The experiments were

performed at temperature (303–333) K, pressure (120–300) bar, and the mass flow rate (0.7–1.2) kg/h. The distilled technical CNSL was having cardanol (78%), cardol (8%), and polymeric material (2%), and 12 % of contents is made of other residual substances. The oils samples were analyzed using GCMS and FTIR. GCMS [15] analysis was done to determine the alkyl-phenols and additional tropical compounds in raw and roasted cashew nut oils obtained by cold processing. The oil obtained from roasted cashew nut has a higher concentration of cardanols. Moreover, HPLC was used to determine the tocopherols. The performance of the 4-stroke diesel engine was evaluated [16] by using the cashew nut shell oil as fuel by direct injecting and additional camphor oil blending. The mixture of cashew nut shell oil (70%) and camphor oil (30%) was called CMPRO 30, providing performance closer to a diesel engine. The brake thermal efficiency is achieved 29.1 %, whereas diesel has shown an efficiency of 30.14%. At full load, the NO emissions of diesel fuel and CMPRO 30 blend are 1068 ppm and 1040 ppm respectively. The NO emission is observed a little bit higher than diesel. The biofuel was generated using CNSL [17] and experimentally verified the performance in a single cylinder, diesel engine working at 1500 rpm. The thermal-cracked CNSL was derived using Cardonal in the temperature range of 180 °C and 380 °C and the performance of the oil was compared with diesel to estimate density, flash point, boiling point, cetane index, calorific value, and kinematic viscosity [18-19]. The separation was discussed of the glucose and fructose sugars of the cashew [20] juice, which is widely used in the purification, concentration, and separation of bio-products. It was investigated [21] the exaction of CNSL using supercritical carbon dioxide (CO₂). The chemical and physical properties of the oil are improved after the supercritical fluid extraction process. The effect of alumina nanoparticles was studied properties on engine performance [22] and emission characteristics of cashew nut shell biodiesel. It is observed that the brake thermal efficiency of CNSL fuel has dropped by 1.1% in comparison to diesel fuel. The parameters HC, CO, NO_x, and smoke were reduced by 7.4%, 5.3%, 10.23%, and 16.1% respectively of CNSL fuel. The sugar fermented-derived bio-products were used to improve the enzymatic digestibility [23] of cashew apple bagasse (CAB) feedstock. The behavior was characterized using NMR, FTIR, and chemical processing. Cashew's nutshell performance of biodiesel was evaluated based on carbon monoxide emissions, carbon dioxide emissions, and brake thermal efficiency [24]. The ignition characteristics of cashew nut shell biodiesel along with ethyne (acetylene) worked as dual fuel in diesel engines. An ethyne-biodiesel mixture in comparison to neat biodiesel examined higher thermal efficiency. The separation technique was used for CNSL from the pericarp [25] of the cashew nut in which supercritical carbon dioxide (CO₂) in 40 – 60°C, and pressures from 14.7 to 29.4 MPa. The extracted CNSL was of light brownish pink color and revealed no confirmation of polymerization or degradation. The cardanols, anacardic acids, and cardols are the components in cashew apple, raw and roasted cashew nut [26]. The CNSL was analyzed using GCMS and NMR [27]. The energetic characteristics of the cashew nut husk and emphasized its utilization as biofuel. The agro residue properties were studied to understand contiguous and essential requirements with advanced heating value. The observed results are bulk density (294 kg/m³) and energy density 5200 (MJ/m³). The double stage trans-esterification

process was used extracted CNSL to synthesize CNSL [28] biodiesel. In the experimental study, it was analyzed that the BTE of the engine was enhanced by 6 % in comparison to the coated engine. The emission [29] of HC, CO, and smoke was reduced by 7.2%, 27.7%, and 14.3%, respectively in full condition, whereas NO_x emission was increased.

Based on the review of different research work in this area, it is identified that a lot of work is done in this domain about the utilization of CNSL as biodiesel and further evaluating the CI engine performance based on performance, combustion, and environment emission parameters. Some researchers have worked on the blended fuel in which some percentage of diesel and the remaining part of CNSL is used to evaluate the performance of the engine under different load conditions. Recently the work is also done in the direction to investigate the effect of diethyl ether with hydrogen to get the enriched performance of CNSL biodiesel in the direct injection diesel engine. The sample is processed on Frontier FTIR apparatus, Perkin Elmer, and GC-MS (CLARUS SQ8S) Perkin Elmer, to determine function groups. In our presented work, the thermal-cracked (TC) CNSL oil is used in blended mode. The TC-CNSL is blended with diesel and used directly without modification in the engine. The blended biodiesel is given as B25 (25 % TC-CNSL and 75 % diesel), B50 (50 % TC-CNSL and 50 % diesel), B75 (25 % TC-CNSL and 25 % diesel) and B100 (100 % TC-CNSL). The main objective of the research paper is to study the behavior of TC-CNSL blended B25, B50, B75, and B100 biodiesel and evaluate the engine based on emission parameters. The LabVIEW software-based GUI is used to get the data for the engine performance calculations. The controller is programmed using embedded 'C' programming in an open ECU system.

2. MATERIALS AND METHODS

2.1 Biodiesel Preparation

The raw cashew nut oil is purchased from Khari Baoli market Delhi, India, and experimentally processed to get thermal-cracked (TC) CNSL. The first step is the processing of raw CNSL using the distillation in which the components are in the proportion of cardanol (78%), cardol (8%), polymeric material (2 %), and other components in the required volume. The work is carried out to derive the thermal-cracked (TC) CNSL oil from Cardonal in the temperature range 150°C to 400°C under 1 bar environmental pressure. The schematic process is depicted in Figure 1. The foremost units of the reactor are the CNSL tank, drain coke, thermocouple, temperature controller, heating coil, pressure gauge, safety valve, beaker, and condenser.

A tank occupied by a 5-liter capacity of cardanol is used in the process. The electric heater heats the reactor by controlling its temperature and the maximum permitted temperature is 400°C. As the evaporated oil is condensed in the condenser, reserved properly in the beaker. The collected oil is thermal cracked (TC) CNSL, looks light-dark in color. The coolant is placed inside the condenser, which is maintained using a continuous flow of water. The pressure is maintained using both pressure gauge and safety valve inside a reactor to limit the pressure and determine the extra pressure produced inside the reactor independently. The thermocouple sensor measures the temperature at one junction where two wires of different materials copper and iron are welded together at one junction.

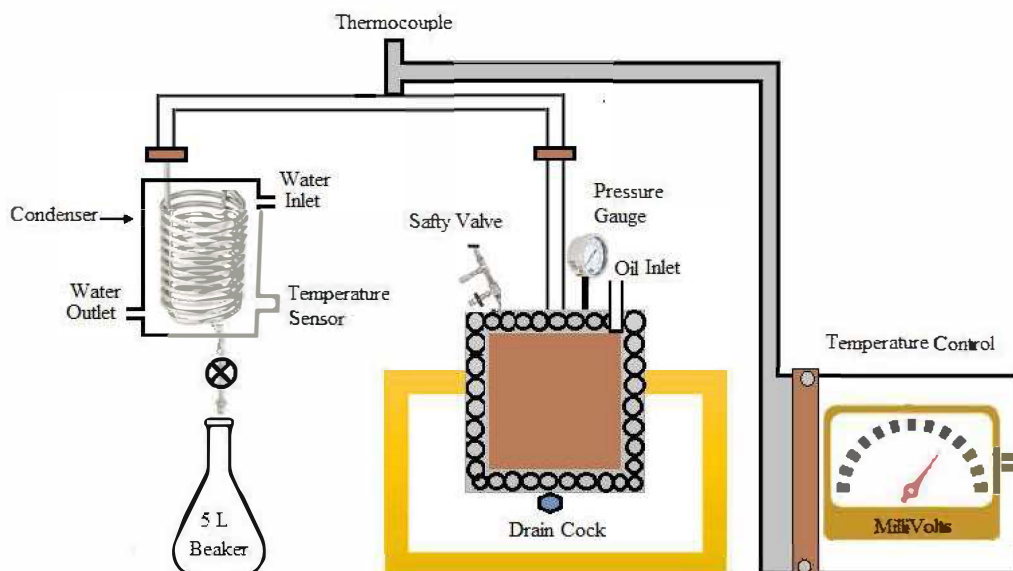


Figure 1. Schematic of TC-CNSL Process [17]

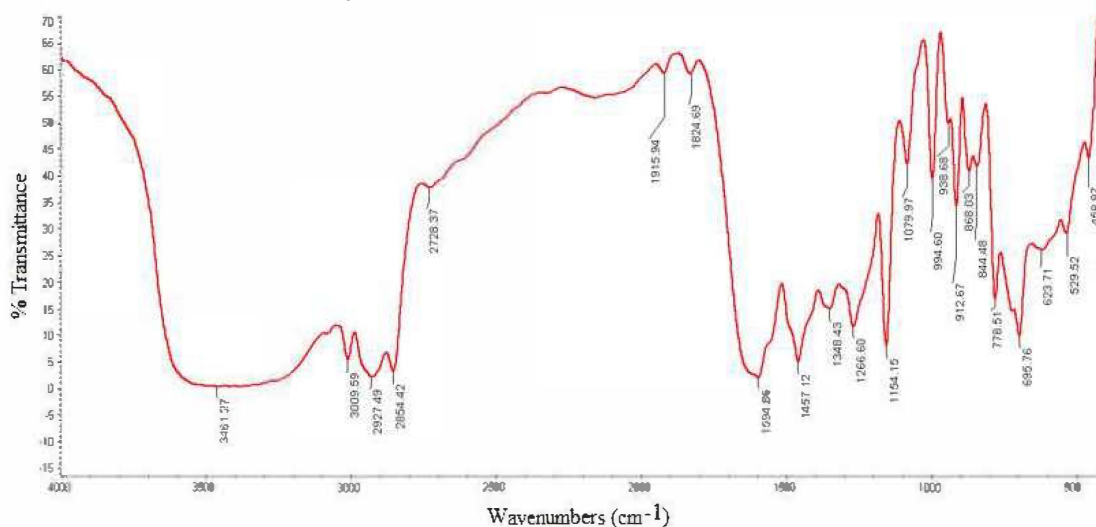


Figure 2. FTIR Analysis of TC-CNSL

1.2 FTIR Spectroscopy

The sample of the TC-CNSL is processed for FTIR spectrometry on Frontier FTIR apparatus, Perkin Elmer. The 'X' axis presents the wavelength (cm^{-1}) and the 'Y' axis presents percentage transmittance [30]. The FTIR spectrum of TC-CNSL is presented in Figure 2 that includes different wavelengths against different functional groups. The spectrum exists in the absorption bands of $4000\text{--}440\text{ cm}^{-1}$. The 1st broad absorbance peak of O–H widening vibration between 3600.00 cm^{-1} and 3009.59 cm^{-1} , which presents phenolic compounds, presents the existence of water impurities and other polymers (O–H) in the oil. The durable absorbance peak of (C–H) vibrations between 2927.49 cm^{-1}

and 2654.42 cm^{-1} , presents the existence of alkanes. The wavelength 1594.86 cm^{-1} : 1154.15 cm^{-1} presents (C–H) deformation vibrations for aldehydes and ketones. The existence of (O–H) and stretching vibrations denotes the presence of carboxylic acids and their possible derivatives esters. The absorbance peaks between 1594.86 cm^{-1} : 1154.15 cm^{-1} present the probable presence of alkenes.

The available peaks between 1266.60 cm^{-1} and 695.76 cm^{-1} are due to the occurrence of primary, secondary, and tertiary alcohols, phenols, ethers, and esters presenting the (O–H) deformation and (C–O) stretching vibration.

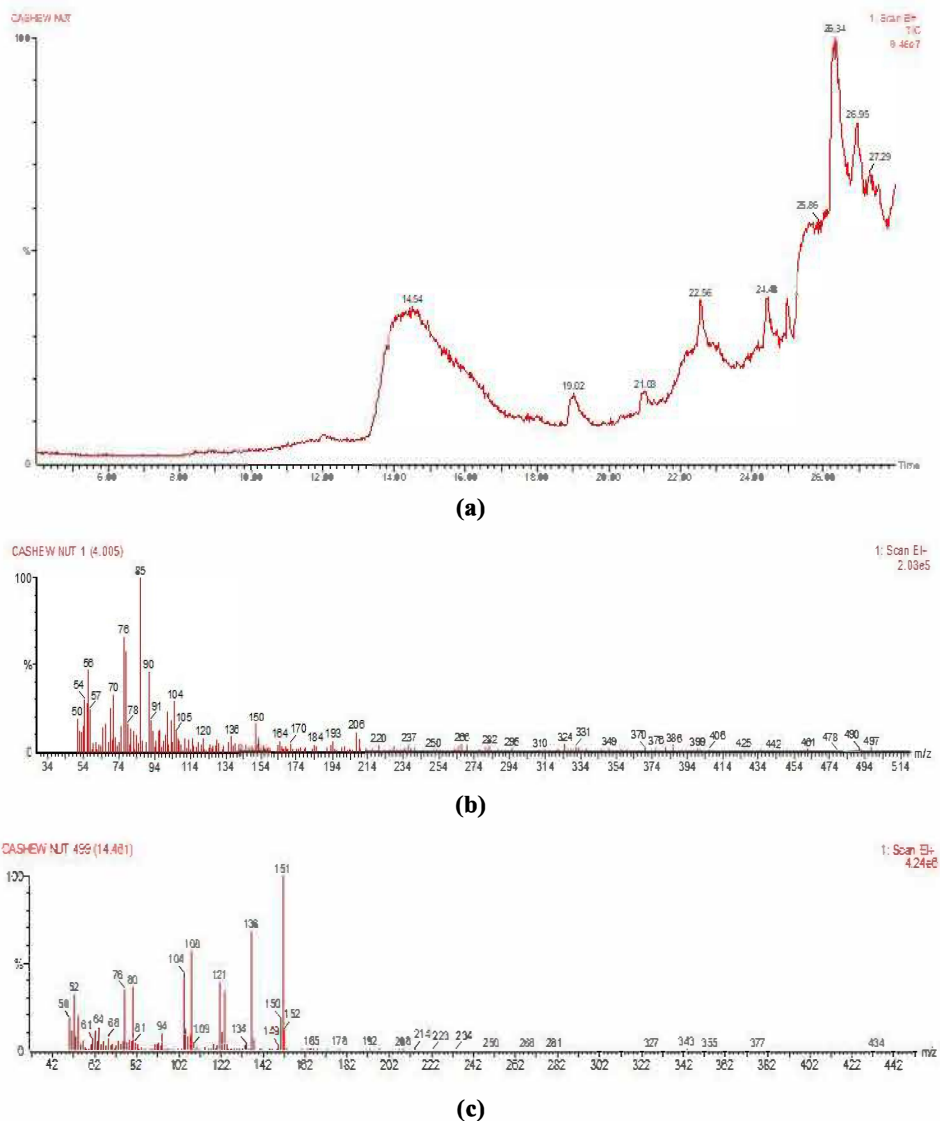


Figure 3. GCMS analysis of TC- CNSL

Table 1. Compounds of GCMS analysis of TC- CNSL

| Hit | Rev | For | Compound Name | M.W | Formula | CAS | Library |
|-----|-----|-----|--|-----|---|-------------|---------|
| 1 | 766 | 544 | BENZALDEHYDE, 2-AMINO-5-METHOXY- | 151 | C ₈ H ₉ O ₂ N | 26831-52-7 | Nist |
| 2 | 734 | 474 | PHENOL, 3-(ETHYLAMINO)-4-METHYL- | 151 | C ₉ H ₁₃ ON | 120-37-6 | Nist |
| 3 | 718 | 531 | 4-METHOXYFORMANILIDE | 151 | C ₈ H ₉ O ₂ N | 5470-34-8 | Nist |
| 4 | 699 | 593 | N-ETHYL-3-METHOXYANILINE | 151 | C ₉ H ₁₃ ON | 41115-30-4 | Nist |
| 5 | 687 | 465 | PHENOL, 3-(ETHYLAMINO)-4-METHYL- | 151 | C ₉ H ₁₃ ON | 120-37-6 | Nist |
| 6 | 668 | 402 | 2-(N-METHYL-N-ETHYLAMINO)PHENOL | 151 | C ₉ H ₁₃ ON | 23504-11-2 | Nist |
| 7 | 632 | 347 | N-ETHYL-P-AMINOPHENOL, N,O-DIACETYL DERI | 221 | C ₁₂ H ₁₅ O ₃ N | 529-94-2 | Nist |
| 8 | 605 | 365 | PYRROLIDINE, 1-(1-CYCLOHEXEN-1-YL)- | 151 | C ₁₀ H ₁₇ N | 1125-99-1 | Nist |
| 9 | 602 | 404 | AMINOCARB | 208 | C ₁₁ H ₁₆ O ₂ N ₂ | 2032-59-9 | Nist |
| 10 | 601 | 452 | 3-METHOXY-5-NITROSALICYLALDEHYDE | 197 | C ₈ H ₇ O ₅ N | 17028-61-4 | Nist |
| 11 | 600 | 456 | ACETAMIDE, N-(4-ACETOXY-3-ACETYLPHENYL)- | 235 | C ₁₂ H ₁₃ O ₄ N | 900280-82-8 | Nist |
| 12 | 583 | 335 | PROPIONAMIDE, 3-(4-FLUOROPHENYL)-N-(4-ME | 301 | C ₁₈ H ₂₀ O ₂ NF | 900311-20-3 | Nist |
| 13 | 559 | 421 | 3-METHOXY-5-NITROSALICYLALDEHYDE | 197 | C ₈ H ₇ O ₅ N | 17028-61-4 | Nist |

| | | | | | | | |
|----|-----|-----|--|-----|--|-------------|-------|
| 14 | 542 | 363 | BENZONITRILE, 2-FLUORO-6-METHOXY- | 151 | C ₈ H ₆ ONF | 94088-46-7 | Ni st |
| 15 | 540 | 349 | BENZOIC ACID, 3-NITRO-, 4-NITROBENZYL ES | 302 | C ₁₄ H ₁₀ O ₆ N ₂ | 144866-85-3 | Nist |
| 16 | 540 | 364 | TROPIDINE, 2-ACETYL-8-DEMETHYL- | 151 | C ₉ H ₁₃ ON | 900128-22-0 | Nist |
| 17 | 518 | 340 | PYRROLIDINE, 1-(1-CYCLOHEXEN-1-YL)- | 151 | C ₁₀ H ₁₇ N | 1125-99-1 | Nist |
| 18 | 507 | 316 | PHENYLTHIOACETIC ACID, 4-ISOPROPYLPHENYL | 286 | C ₁₇ H ₁₈ O ₂ S | 900331-22-3 | Nist |
| 19 | 498 | 342 | 1-(PHENYLTHIO)-3-(2-PYRIDINYLOXY)-2-PROP | 259 | C ₁₄ H ₁₃ O ₂ NS | 900326-75-8 | Nist |
| 20 | 494 | 352 | 2-(METHYLTHIO)BENZOIC TRIFLUOROACETIC AN | 264 | C ₁₀ H ₇ O ₃ F ₃ S | 900374-99-3 | Nist |

2.3 GCMS Analysis

GC-MS (CLARUS SQ8S Perkin Elmer) set up is one of the fast quadrupole mass spectrometers, works on the large spectra (12,500 amu/sec) against each GC peak. It supports the quantification of exceptionally narrow chromatographic peaks and provides clear definitions for precise and exceptional data. This instrument also provides the largest mass range accessible in gas chromatography (1-1200 u) and finding limits, not possible to meet in single quadrupole GC/MS. The mass spectrometer is set to work in the electron impact (EI) mode of ionization and scan the results in the range of 50–550 (m/z) with peaks. The initial oven temperature is kept at 60°C for 2.25 min, followed by an incremental rate of 6° per minute, up to 350°C.

Figure 3 presents the GCMS of TC-CNSL on the different time scales. The X-axis denotes the retention time, ratio of mass to charge (m/z) and Y-axis denotes the signal intensity (abundance) against each ion. Table 1 presents the chemical characterization of available compounds with a chemical formula such as linear, saturated, or unsaturated chains and oxygenated products.

3. PROPERTIES OF TC-CNSL BIODIESEL

Table 2 lists the comparative properties of diesel, raw CNSL, and obtained TC-CNSL biodiesel based on the physicochemical characteristics: Density (ASTM D 4052), kinematic viscosity (ASTM D 445), flash point (ASTM D 93), calorific value (ASTM D 240), cetane index (ASTM D 976),

boiling point (ASTM D 1160), pour point (ASTM D 97) and acid value (ASTM D 664).

Table 2. Properties of diesel, CNSL obtained TC-CNSL biodiesel

| Parameters | Diesel | Raw CNST | TC- CNST |
|---------------------------------------|---------|----------|----------|
| Density at 15 °C (Kg/m ³) | 814.00 | 908.00 | 829.00 |
| Kinematic viscosity at 40 °C (cSt) | 2.57 | 16.10 | 5.70 |
| Flash Point (°C) | 50.00 | 214.00 | 115.00 |
| Calorific value (kJ/kg) | 42500 | 35800 | 40150 |
| Cetane Index | 45-55 | 33 | 30 |
| Boiling Point (°C) | 180-340 | 225 | 210 |
| Pour Point (°C) | -29 | -12 | -2 |
| Acid Value (mgKOH/gm) | 21.3 | 13.2 | 2.17 |

The properties of the TC-CNSL is also compared with existing work by Velmurugan et al. [31] Vedharaj et al [28], Loganathan, et al. [19] Kasiraman [16] Senthil et al. [24] Bangjang et al. [12] and Devaraj et al. [32]. Table 3 presents the comparative properties of the TC-CNSL in existing research papers. It is also observed that most of the properties are optimal in comparison to other’s work.

Table 3. Comparison with existing work

| Parameters | Loganathan, et al. [19], Velmurugan et al. [31] | Vedharaj et al. [28] | Kasiraman et al. [16] | Senthil et al. [24] | Bangjang et al.[12] | Devaraj et al. [32] | Biodiesel CNST |
|---------------------------------------|---|------------------------|-----------------------|---------------------|---------------------|---------------------|----------------|
| Density at 15 °C (Kg/m ³) | 821 | 909.3 | 958.1 | 906.4 | 846 | 882.4 | 829.00 |
| Kinematic viscosity at 40 °C (cSt) | 4.43 | 10.3× 10 ⁻⁶ | 55.3 | 10.3 | 2.85 | 4.28 | 5.70 |
| Flash Point (°C) | <28 | 170 | 234 | 66 | - | 139 | 115.00 |
| Calorific value (kJ/kg) | 41780 | 34300 | 35800 | 38400 | 40670 | 38113 | 40150 |
| Cetane Index | 45 | 41 | 33 | 50 | 48 | - | 30 |
| Boiling Point (°C) | 180-380 | - | - | - | - | - | 210 |
| Pour Point (°C) | - | -1 | - | - | -2 | - | -2 |
| Acid Value (mgKOH/gm) | - | 3.69 | - | - | 0.78 | - | 2.17 |

3.1 Blending Nano Additives

The TC-CNSL is blended with diesel and Cerium Oxide Nanoparticles. TC- CNSL and No.2 diesel are blended in a ratio (25:75), called B25, and 25 ppm cerium oxide nano

additive is added to B25, called B25 + C25. The 50 ppm cerium oxide nano additive is added to the B25 blend and is called B25 + C50. In the same way, the 50 ppm Cerium Oxide Nanoparticles are added in the blended fuel B25, B50, B75, and B100. The essential amount of the nanoparticle is

measured using a precision electronic balance and added to the fuel using a mechanical agitator, with a constant agitation time of 15 minutes to make a constant suspension. The blends are used instantly, after preparation, to avoid any settling. The Cerium oxide nanoparticles are cost-effective and sustain their catalytic behavior under tough conditions. The nanostructures of cerium oxide change the oxygen non-stoichiometry ratio of Ce^{3+}/Ce^{4+} on the surface of nanostructures. The Cerium oxides have the features to act as an oxygen buffer that affects the immediate oxidation of hydrocarbons as well as the reduction of oxides of nitrogen, thus reducing emissions, especially in stoichiometric environments. The nanoparticles exhibit high catalytic movement as the large surface area exists per unit volume, which mainly increases the fuel efficiency and decreases emissions.

4. EXPERIMENTAL STUDY

The experimental setup is shown in Figure 4. A single-cylinder, four-stroke, water-cooled Common Rail Direct Injection (CRDI) diesel engine of company Kirloskar (AV1 5 HP) is used for this work. It has the bowl in the piston crown assist as the combustion chamber. The engine has the specifications: water-cooled, direct-injected, 4 strokes, single-cylinder, compression ratio: 16.51, fuel tank capacity: 6.5 L, cubic capacity: 0.553 L, Bore (mm) x stroke (mm): 80 mm x 110 mm, rated speed: 1500 rpm, torque: 2.387 Kg-m, injection pressure: (0-200) bar, Injection timing: 21° bTDC, injection type: electronic fuel injector, crankshaft center height: 203 mm, size of bare engine: (617 mm x 504 mm x 843 mm,) engine weight: 130 Kg, overload capacity: 10% of rated power, power take-off: flywheel end. The default values of injection time and injection pressure are kept based on the manufacture datasheet. The engine maintains the rated speed of 1500 rpm on 220 V supply voltage and constant supply frequency (50 Hz) with a rated power of 4 KW. In the detailed CDRI engine, the pressure can be increased up to 200 MPa bar inside the fuel injection system. In the experiment, the best performance of the system is observed at 200 bar for the constant speed of 1500 rpm and variation loads. The engine has a top crank center position at which the piston is on rest, senses the crank angle when cylinder volume is minimized and picks up the pulse. An eddy current dynamometer is placed in the engine to work under different loads and measures the engine power output against these different loads. During this process, the fuel pump rack position is attuned to conserve a constant speed of 1500 rpm.

The Engine Management System (EMS) is associated with Engine Control Unit (ECU) with the help of a CAN converter, used to control engine injection through program control such as injection quantity, injection timing, split injection percentage, and communication with the engine. The open ECU system has a guidance service suggestion (GSS) function, its primary module is designed using Embedded 'C' programming, and LabVIEW programming-based GUI interface. The LabVIEW (RT) has an ECU measurement calibration toolkit that supports CAN protocol. The high-speed data acquisition system (DAS) is used to measure the quantity

of different pressure, temperatures in the fuel line, exhaust gas line, water cooling line and record the pressure data associated with crank angle. The data acquisition card transfers the data to the computer. The diesel and air utilization measurements were acquired from pressure transmitter interfaced instruments.

The dedicated LabVIEW software-based GUI is developed to get the data for the engine performance calculations from suitable hardware units so that the transducers and sensors can provide the necessary input data to the system software. A piezoelectric transducer works as a pressure sensor used for sensing in-cylinder pressure (0-200 bar) and is attached to the engine cylinder. The LabVIEW-GUI interface measures and record the cylinder pressure data. The exhaust emissions such as CO, NO_x, HC, and CO₂ are measured with the help of the AVL five gas analyzer under different loads on the engine. The exhaust gas sample line is retained at 190°C and the smoke emission meter measures smoke density. The smoke is measured using a standard AVL 437C smoke meter that works on the principle of light extinction. To achieve better accuracy, the reading is taken three times and the average value is considered.

The uncertainty analysis is done based on the methods suggested by Holman [33] and Moffat. The errors of various parameters are based on the principle of propagation of errors. It is originated from operating conditions, observations, environment, and instrument selection. Table 4 lists measurement uncertainty. The percentage uncertainties of brake power (0.605 %), BSFC (0.600 %), and BTE (0.600 %) were calculated using the percentage uncertainties of various instruments used in the experiment.

Table 4. Measurement Uncertainty

| Measurement | Accuracy | % Uncertainty |
|------------------------------|----------|---------------|
| Load | ±10 N | ±0.2 |
| Burette for fuel measurement | ±0.2 cc | ±1.5 |
| Speed | ±10 rpm | ±0.1 |
| Manometer | ±1 mm | ±1.0 |
| Time | ±0.1 s | ±0.2 |
| CO | ±0.03% | ±1.0 |
| HC | ±15 ppm | ±0.2 |
| NO _x | ±15 ppm | ±0.2 |

5. RESULTS AND DISCUSSIONS

The 50 ppm Cerium Oxide nanoparticles are added uniformly. The blended B25 + C50, B50 + C50, B75 + C50 and B100 + C50 is read as B25, B50, B75 and B100. The biodiesel study can be carried out based on emission parameters such as emission of CO₂, CO, HC, and NO_x [34].

5.1 CO Emissions

Figure 5 presents the variation of CO and brake mean effective pressure (BMEP) in diesel and blended TC-CNSL biodiesel at part load and full load.

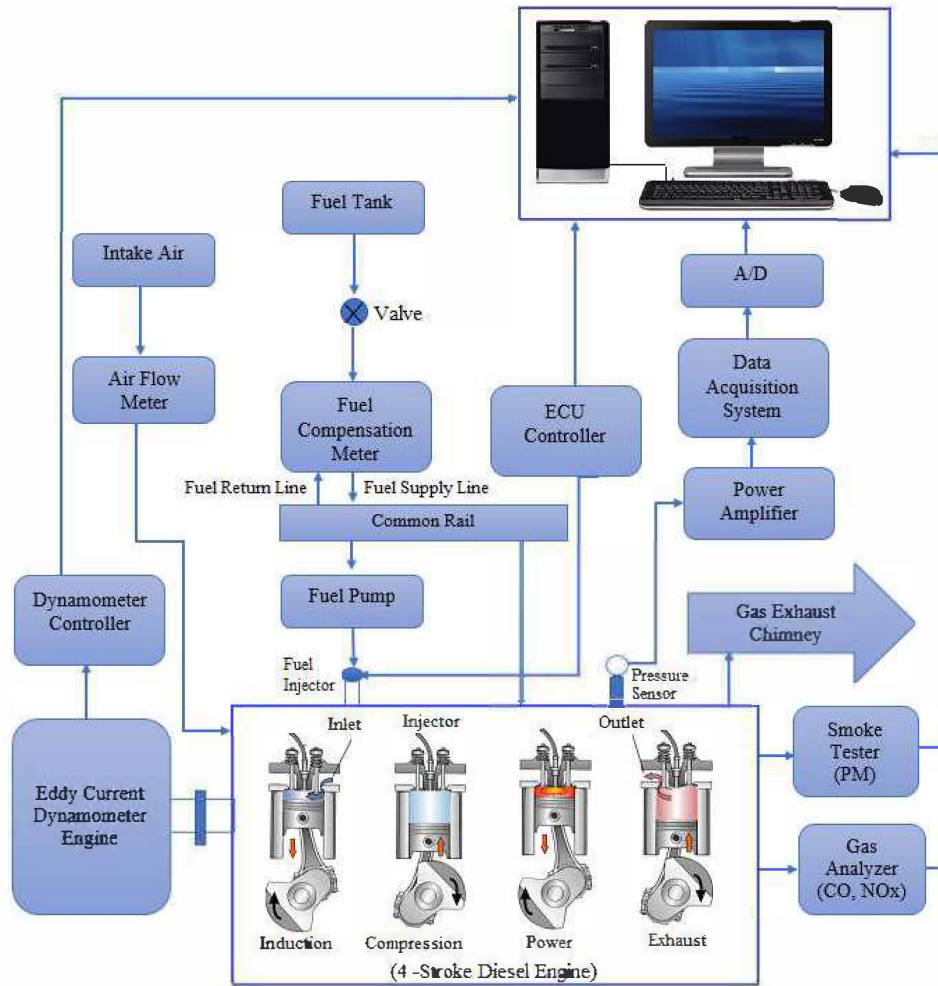


Figure 4. Schematic of the experimental setup

The CO emission is a function of temperature and availability of Oxygen. Generally, diesel engine runs on a lean mixture that causes lower CO emissions. The variations in CO are due to incomplete combustion, due to improper mixing, lower oxygen content, poor air-fuel ratio, lack of time for reaction and mixing.

It is observed that the CO emission of all blended TC-CNSL is lower than diesel at all loads. The percentage reduction of CO is 10.2%, 18.1%, 30.00% and 40.5 % for B-25, B-50, B-75, and B-100 respectively, compared to diesel fuel. At part load, the CO emissions are lower in the initial phase of combustion. The 50-60% heat is released in the initial phase of combustion in which ions and radicals are coming out that maintain lower emissions. At the full load, more CO is emitted as the combustion process is completed.

5.2 CO₂ Emissions

Figure 6 presents the variation of CO₂ and brake mean effective pressure (BMEP) in diesel and blended TC-CNSL biodiesel at part load and full load. It is observed that CO₂ emission is increasing for both diesel and biodiesel, with the variation of load. The blended TC-CNSL experienced less CO₂ emission in comparison to diesel. The percentage

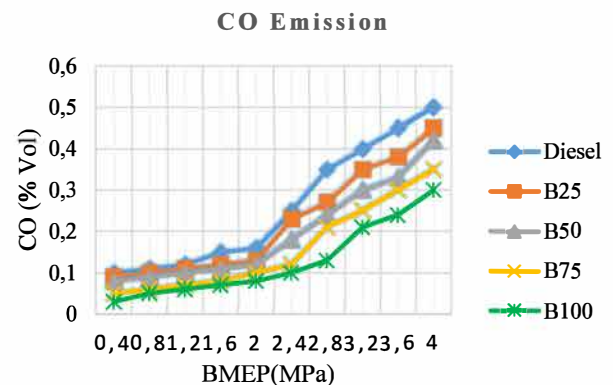


Figure 5. Variation of CO emissions with load

reduction of CO₂ is 6.25%, 29.7%, 40.62% and 60.9 % for B-25, B-50, B-75, and B-100 respectively, compared to diesel fuel. The combustion time is slightly increased during fuel injection that affects the amount of CO₂ variation.

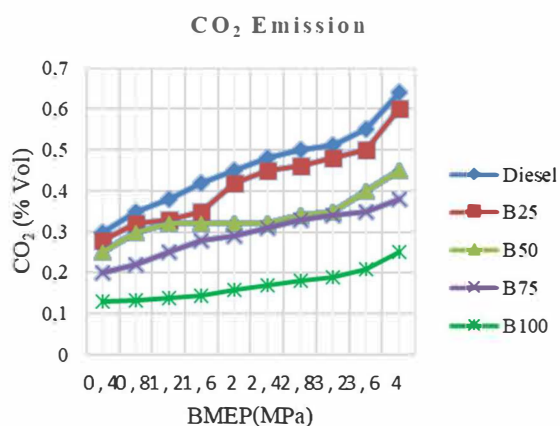


Figure 6. Variation of CO₂ emissions with load

5.3 Hydrocarbon (HC) Emissions

In the diesel engine, the reason for liberation of HC emissions can be due to numerous factors, such as unburned fuels in lower temperature near cylinder wall, fuel properties, excessive dilution with air, wall quenching, higher fumigation rate, and fuel that vaporizes from the nozzle sac in the last duration of combustion. The unburned hydrocarbon is the straight outcome of incomplete combustion in the combustion chamber. The Hydrocarbons comprise thousands of species, such as alkenes, alkanes, and aromatics [35], and are usually specified in terms of equivalent CH₄ contents. Figure 7 presents the HC emissions in diesel and blended TC-CNSL biodiesel at part load and full load.

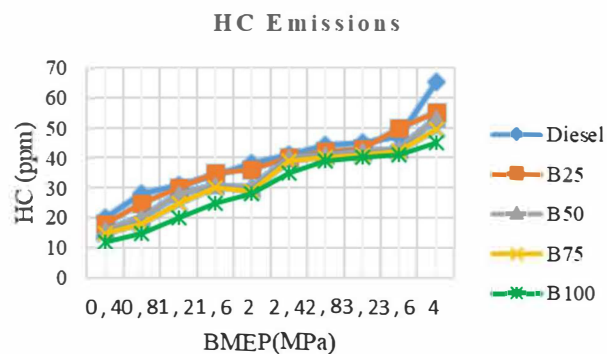


Figure 7. HC variation with brake mean effective pressure

The HC emissions for diesel are 65 ppm at full load. The observed HC emissions for B-25, B-50, B-75, and B-100 are 55.10, 53.00, 49.50, and 44.9 ppm respectively, at full load. Therefore, there is a reduction of 30% HC emissions of B-100 in comparison to diesel at full load. The same behavior is also analyzed at part load in which a 16 % reduction is observed for B-100 in comparison to diesel.

5.4 Oxides of Nitrogen (NOx) Emissions

The variation on NO_x is due to lower viscosity, higher oxygen contents, and reduction in combustion temperature that affects the oxidation process [36-37]. Figure 8 presents the NO_x emissions and brake means effective pressure (BMEP) in diesel and TC-CNSL biodiesel at part

load and full load. The variation on NO_x is due to two factors: the maximum temperature of the cylinder and the quantity of oxygen in fuel composition. The observed NO_x emissions are 575.0, 601.4, 626.3, 637.2, and 640.2 for diesel, B-25, B-50, B-75, and B-100 respectively, at full load. It is clarified that blended TC-CNSL is having more NO_x emission in comparison to diesel at full load. The B100 is emitting 9.23 % and 11.26 % larger emissions in comparison to diesel at part load and full load respectively.

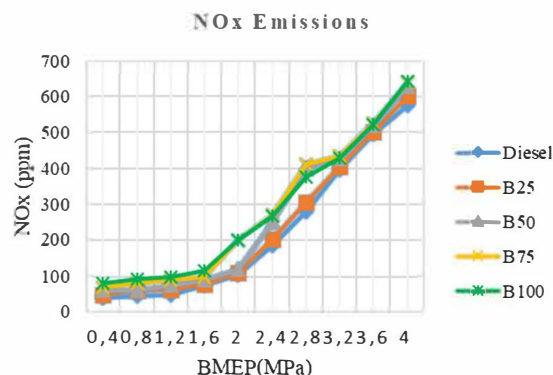


Figure 8. NO_x variation with brake mean effective pressure

5.5 Smoke Intensity

Smoke emissions are nothing but the exhaust gas stream [38] in which the solid soot stems are deferred. Figure 9 shows that the smoke emissions are increasing for both diesel and blended biodiesel with different engine loads due to incomplete combustion of fuel. The diesel engine emits smoke due to poor injector maintenance, poor driving mechanism [39-40], and excessive fuel delivery rates. If the engine smoke emissions are more, it means that the engine is wasting fuel and leading to damage. The measured smoke intensity is 3.65, 3.60, 3.52, 3.42, and 3.21 BSU for diesel, B-25, B-50, B-75, and B-100 respectively, at full load. It is clarified that smoke intensity is decreasing in blended TC-CNSL biodiesel in comparison to diesel.

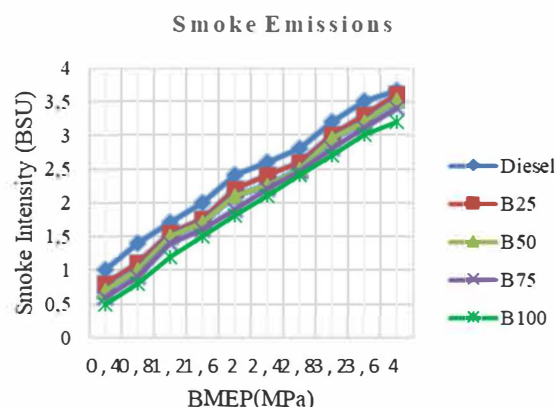


Figure 9. Smoke emissions variation with brake mean effective pressure

6. CONCLUSIONS

Cashew nut shell liquid (CNSL) biodiesel is obtained using thermal-cracked TC-CNSL oil processing from Cardonal in

the temperature range 150°C to 400°C. The properties of TC-CNSL biodiesel are analyzed based on ASTM standards: density (829.0 kg/m³ at 15°C), kinematic viscosity (5.70 cSt at 40°C), flash point (115°C), calorific value (40150 KJ/Kg), cetane index (30), boiling point (210°C), pour point (-2°C) and acid value (2.17 mgKOH/gm). The following results are studied by adding the Cerium Oxide Nanoparticles with blended TC-CNSL-B25, TC-CNSL-B50, TC-CNSL-75, and TC-CNSL-B100.

- It is observed that the CO emission of all blended TC-CNSL is reduced by 10.2%, 18.1%, 30.00% and 40.5 % for all blended TC-CNSL B-25, B-50, B-75, and B-100 respectively, in comparison to diesel fuel. In all observations, the CO emissions are less than diesel in blended TC-CNSL. At part load, the CO emissions are lower in the initial phase of combustion.
- The CO₂ emissions are reduced in all the blended TC-CNSL fuel. The percentage reduction of CO₂ is 6.25%, 29.7%, 40.62% and 60.9 % in B-25, B-50, B-75, and B-100 respectively, in comparison to diesel fuel.
- The HC emissions are reducing in blended TC-CNSL, in comparison to diesel, at full load. The observed values of HC emissions are 65.00, 55.10, 53.00, 49.50, and 44.9 ppm for diesel, B-25, B-50, B-75, and B-100 respectively, at full load. HC emissions of B-100 are reduced by 30.7 % in comparison to diesel, at full load.
- The NO_x emissions are increasing in blended TC-CNSL, in comparison to diesel, at full load. The observed NO_x emissions are 575.0, 601.4, 626.3, 637.2, and 640.2 for diesel, B-25, B-50, B-75, and B-100 respectively, at full load. The NO_x emissions are increased by 11.26 % in B-100 in comparison to diesel, at full load.
- The smoke intensity is decreasing in blended TC-CNSL, in comparison to diesel, at full load. The measured smoke intensity is 3.65, 3.60, 3.52 3.42, and 3.21 BSU for diesel, B-25, B-50, B-75, and B-100 respectively, at full load.

REFERENCES

- [1] Senthil Kumar, D., Thirumalini, S. (2020). Investigations on effect of split and retarded injection on the performance characteristics of engines with cashew nut shell biodiesel blends. *International Journal of Ambient Energy*, 1-9.
- [2] Anand, O. N., Chhibber, V. K. (2006). Vegetable oil derivatives: environment-friendly lubricants and fuels. *Journal of Synthetic Lubrication*, 23(2):91-107.
- [3] Bhatnagar, A. K., Kaul, S., Chhibber, V. K., Gupta, A. K. (2006). HFRR studies on methyl esters of nonedible vegetable oils. *Energy Fuels*, 20(3), 1341-1344.
- [4] Agarwal, A. K. (2007). Biofuels (alcohols and biodiesel) applications as fuels for internal combustion engines. *Progress in energy and combustion science*, 33(3): 233-271.
- [5] Agarwal, D., Agarwal, A. K. (2007). Performance and emissions characteristics of *Jatropha* oil (preheated and blends) in a direct injection compression ignition engine. *Applied thermal engineering*, 27(13): 2314-2323.
- [6] Agarwal, A. K., Singh, A. P., Thipse, S. S., Goswami, G. (2021). A Review on Energy, Environment, and Emissions Issues in Indian Road Transport Sector. *Transactions of the Indian National Academy of Engineering*, 1-17.
- [7] Kumar, D., Chhibber, V. K., Singh, A. (2017). Review of Vegetable Seeds Oils as Biolubricants. *Energy and Environment Focus*, 6(2): 103-113. doi: 10.1166/eef.2017.1251.
- [8] Tan, L. N., Carlton, R., Cleaver, K., Abbott, N. L. (2014). Liquid crystal-based sensors for rapid analysis of fatty acid contamination in biodiesel. *Molecular Crystals and Liquid Crystals*, 594(1): 42-54.
- [9] Patel, R. N., Bandyopadhyay, S., Ganesh, A. (2011). Extraction of cardanol and phenol from bio-oils obtained through vacuum pyrolysis of biomass using supercritical fluid extraction. *Energy*, 36(3):1535-1542.
- [10] Lomonaco, D., Mele, G., Mazzetto, S. E. (2017). Cashew nutshell liquid (CNSL): from an agro-industrial waste to a sustainable alternative to petrochemical resources. In *Cashew Nut Shell Liquid* (pp. 19-38). Springer.
- [11] Facanha, M.A.R., Mazzetto, S.E., Carioca, J.O.B., de Barros, G.G. (2007). Evaluation of antioxidant properties of a phosphorated cardanol compound on mineral oils (NH10 & NH20). *Fuel*, 86(15):2416-2421.
- [12] Bangjang, T., Saisangtong, R., Kaewchada, A., Jaree, A. (2014). Modification of diesohol fuel properties by using cashew nut shell liquid and biodiesel as additives. *Energy Technology*, 2(10):825-831.
- [13] Solanki, J. H., Javiya, T. V. (2012). Cashew Nut shell liquid fuel an substitute for diesel fuel to be used in CI engine. *International Journal of Advance Research in Science, Engineering and Technology*, 1(2):8-12.
- [14] Gangil, S. (2014). Dominant thermogravimetric signatures of lignin in cashew shell as compared to cashew shell cake. *Bioresource technology*, 155:15-20.
- [15] Gómez-Caravaca, A. M., Verardo, V., Caboni, M. F. (2010). Chromatographic techniques for the determination of alkyl-phenols, tocopherols and other minor polar compounds in raw and roasted cold pressed cashew nut oils. *Journal of Chromatography A*, 1217(47):7411-7417.
- [16] Kasiraman, G., Nagalingam, B., Balakrishnan, M. (2012). Performance, emission and combustion improvements in a direct injection diesel engine using cashew nut shell oil as fuel with camphor oil blending. *Energy*, 47(1):116-124.
- [17] Loganathan, M., Thanigaivelan, V., Madhavan, V. M., Anbarasu, A., Velmurugan, A. (2020). The synergetic effect between hydrogen addition and EGR on cashew nut shell liquid biofuel-diesel operated engine. *Fuel*, 266:117004.
- [18] Loganathan, M., Madhavan, V. M., Balasubramanian, K. A., Thanigaivelan, V., Vikneswaran, M., Anbarasu, A. (2020). Investigation on the effect of diethyl ether with hydrogen-enriched cashew nut shell (CNS) biodiesel in direct injection (DI) diesel engine. *Fuel*, 277:118165.
- [19] Luz, D. A., Rodrigues, A. K. O., Silva, F. R. C., Torres, A. E. B., Cavalcante Jr, C. L., Brito, E. S., Azevedo, D. C. S. (2008). Adsorptive separation of

- fructose and glucose from an agroindustrial waste of cashew industry. *Bioresource technology*, 99(7): 2455-2465.
- [21] Patel, R. N., Bandyopadhyay, S., Ganesh, A. (2006). Extraction of cashew (*Anacardium occidentale*) nut shell liquid using supercritical carbon dioxide. *Bioresource Technology*, 97(6): 847-853.
- [22] Radhakrishnan, S., Munuswamy, D. B., Devarajan, Y., Mahalingam, A. (2018). Effect of nanoparticle on emission and performance characteristics of a diesel engine fueled with cashew nut shell biodiesel. *Energy Sources, Part A: Recovery, Utilization, and Environmental Effects*, 40(20): 2485-2493.
- [23] Reis, C.L.B., E Silva, L.M.A., Rodrigues, T.H.S., Félix, A. K. N., de Santiago-Aguiar, R. S., Canuto, K. M., Rocha, M. V. P. (2017). Pretreatment of cashew apple bagasse using protic ionic liquids: enhanced enzymatic hydrolysis. *Bioresource technology*, 224: 694-701.
- [24] Senthil kumar, G., Sajin, J. B., Yuvarajan, D., Arunkumar, T. (2020). Evaluation of emission, performance and combustion characteristics of dual fueled research diesel engine. *Environmental Technology*, 41(6): 711-718.
- [25] Smith Jr, R. L., Malaluan, R. M., Setianto, W. B., Inomata, H., Arai, K. (2003). Separation of cashew (*Anacardium occidentale* L.) nut shell liquid with supercritical carbon dioxide. *Bioresource technology*, 88(1): 1-7.
- [26] Trevisan, M. T. S., Pfundstein, B., Haubner, R., Würtele, G., Spiegelhalter, B., Bartsch, H., Owen, R. W. (2006). Characterization of alkyl phenols in cashew (*Anacardium occidentale*) products and assay of their antioxidant capacity. *Food and Chemical Toxicology*, 44(2):188-197.
- [27] Torres Gadelha, A. M., Lima Almeida, F. D., Silva, R. A., Malveira, J. Q., Sanders Lopes, A. A., De Sousa Rios, M. A. (2019). Cashew nut husk and babassu coconut husk residues: evaluation of their energetic properties. *Energy Sources, Part A: Recovery, Utilization, and Environmental Effects*, 1-9.
- [28] Vedharaj, S., Vallinayagam, R., Yang, W. M., Chou, S. K., Chua, K. J. E., Lee, P. S. (2014). Experimental and finite element analysis of a coated diesel engine fueled by cashew nut shell liquid biodiesel. *Experimental Thermal and Fluid Science*, 53:259-268.
- [29] Vedharaj, S., Vallinayagam, R., Yang, W. M., Saravanan, C. G., Roberts, W. L. (2016). Synthesis and utilization of catalytically cracked cashew nut shell liquid in a diesel engine. *Experimental Thermal and Fluid Science*, 70:316-324.
- [30] Langer, J. J., Moss, G. P. (1993). FTIR studies of trimethylene linked bis-diacetylene derivatives. *Molecular Crystals and Liquid Crystals Science and Technology. Section A. Molecular Crystals and Liquid Crystals*, 237(1):457-461.
- [31] Velmurugan, A., Loganathan, M., Gunasekaran, E. J. (2014). Experimental investigations on combustion, performance, and emission characteristics of thermal cracked cashew nut shell liquid (TC-CNSL)-diesel blends in a diesel engine. *Fuel*, 132:236-245.
- [32] Devaraj, A., Vinoth Kanna, I., Tamil Selvam, N., Prabhu, A. (2020). Emission analysis of cashew nut biodiesel-pentanol blends in a diesel engine. *International Journal of Ambient Energy*, 1-5.
- [33] Moffat, R. J. (1988). Describing the uncertainties in experimental results. *Experimental thermal and fluid science*, 1(1):3-17.
- [34] Chong, C. T., Chiong, M. C., Ng, J. H., Lim, M., Tran, M. V., Valera-Medina, A., Chong, W. W. F. (2019). Oxygenated sunflower biodiesel: Spectroscopic and emissions quantification under reacting swirl spray conditions. *Energy*, 178:804-813.
- [35] Yamada, H., Misawa, K., Suzuki, D., Tanaka, K., Matsumoto, J., Fujii, M., Tanaka, K. (2011). Detailed analysis of diesel vehicle exhaust emissions: Nitrogen oxides, hydrocarbons, and particulate size distributions. *Proceedings of the Combustion Institute*, 33(2):2895-2902.
- [36] Lapuerta, M., Armas, O., Rodriguez-Fernandez, J. (2008). Effect of biodiesel fuels on diesel engine emissions. *Progress in energy and combustion science*, 34(2):198-223.
- [37] Singh, Y., Garg, R., Kumar, S. (2019). Friction and wear characterization of modified jatropha oil (*Jatropha Curcas*) using pin on disc tribometer. *Energy Sources, Part A: Recovery, Utilization, and Environmental Effects*, 1-12.
- [38] Singh, Y., A. Singla, and A. K. Singh. 2017d. Tribological characteristics of Mongongo-oil-Based biodiesel blended lubricant. *Energy Sources, Part A: Recovery, Utilization, and Environmental Effects* 39(3):332-338.
- [39] De Sousa Rios, M. A., Nascimento, T. L., Santiago, S. N., Mazzetto, S. E. (2009). Cashew nut shell liquid: a versatile raw material utilized for syntheses of phosphorus compounds. *Energy Fuels*, 23(11):5432-5437.
- [40] Kanthavelkumaran, N., Seenikannan, P., Kumaresh, E. (2016). Exhaust measurement and emission control-biodiesel involvement in diesel engine. *Automatika: časopis za automatiku, mjerenje, elektroniku, računarstvo i komunikacije*, 57(2):532-539.

NOMENCLATURE

| | |
|-----------------|---|
| ASTM | American Society for Testing and Materials |
| BMEP | Brake Mean Effective Pressure |
| BSU | Bosch Smoke Unit |
| CAN | Controller Area Network |
| CNSL | Cashew Nut Shell Liquid |
| CO ₂ | Carbon Dioxide |
| CO | Carbon Monoxide |
| DAS | Data Acquisition System |
| ECU | Engine Control Unit |
| EMS | Engine Management System |
| FTIR | Fourier-transform infrared spectroscopy |
| GCMS | Gas-Chromatography-Mass Spectrometry |
| GUI | Graphical User Interface |
| HC | Hydrocarbon |
| HPLC | High Performance Liquid Chromatography |
| LabVIEW | Laboratory Virtual Instrument Engineering Workbench |
| MT-Ha | Million-ton Hectares |

| | |
|-----------------|----------------------------|
| NO _x | Nitrogen Oxide |
| NMR | Nuclear Magnetic Resonance |
| ppm | Parts Per Million |
| TC | Thermal-Cracked |
| rpm | Revolutions per minute |